

Case Report

Diagnosis of Cystic Endometrial Hyperplasia and Hydrometra in a Pet Goat

Ryo Nishimura ¹, Masamichi Yamashita ², Yusuke Murahata ², Yuji Sunden ³  and Takeshi Tsuka ^{2,*} 

¹ Laboratory of Theriogenology, Joint Department of Veterinary Medicine, Faculty of Agriculture, Tottori University, 4-101, Koyama-Minami, Tottori 6808553, Japan; ryon@tottori-u.ac.jp

² Clinical Veterinary Sciences, Joint Department of Veterinary Medicine, Faculty of Agriculture, Tottori University, 4-101, Koyama-Minami, Tottori 6808553, Japan; yamashita@tottori-u.ac.jp (M.Y.); ymurahata@tottori-u.ac.jp (Y.M.)

³ Laboratory of Veterinary Pathology, Joint Department of Veterinary Medicine, Faculty of Agriculture, Tottori University, 4-101, Koyama-Minami, Tottori 6808553, Japan; sunden@tottori-u.ac.jp

* Correspondence: tsuka@tottori-u.ac.jp

Simple Summary: Differential diagnosis is required for uterine diseases in goats because of the variety of pathogenesis. Hydrometra can be effectively differentiated from other uterine diseases using a combination of imaging techniques such as ultrasonography, computed tomography, and hysteroscopy, allowing observation of morphological abnormalities in the uterine contour and inside the uterine lumen and identification of structural abnormalities, including vascularization and inflammation.

Abstract: This case report includes the clinical utility of ultrasonography, intrauterine endoscopy (hysteroscopy), and computed tomography (CT) in the preoperative evaluation of hydrometra in a pet goat, which did not completely heal with medical therapy using prostaglandin F₂α. Ultrasonography revealed an anechoic liquid within the uterine lumen on a percutaneous scan. CT identified an enlarged uterus and right ovary with a cystic follicle-like structure. Hysteroscopy revealed an accumulation of clear fluids within the uterine lumen and a corrugated, thickened endometrial structure. Plasma estradiol-17β (E2) concentrations were found to be higher (41.9 pg/mL) than normal levels, whereas plasma progesterone (P4) concentrations were at normal levels (0.55 ng/mL) during the follicular phase. Histopathological examination of the endometrium removed by biopsy revealed accelerated mucosal secretion with hyperplasia. Ovariohysterectomy was performed 14 days after the initial diagnosis. Immediately before surgery, plasma E2 and P4 levels were 23.4 pg/mL and 18.34 ng/mL, respectively. Histopathological examination of the surgically removed endometrium revealed cystic endometrial hyperplasia in the uterus and follicular cysts in the ovary. Based on these results, the patient was histologically diagnosed with hydrometra, including cystic endometrial hyperplasia, possibly induced by follicular cysts in the ovary. Ultrasonography and intrauterine endoscopy enabled clear visualization of the secreted mucosa within the uterine lumen, whereas CT enabled an effective visualization of an ovary with a cystic follicle structure. Preoperative observations based not only on ultrasonography but also on evaluations, particularly combined with CT and endoscopy, are useful in diagnosing hydrometra and determining the need for ovariohysterectomy in goats.

Keywords: computed tomography; goat; hydrometra; hysteroscopy; ovariohysterectomy



Academic Editor: Emma Bleach

Received: 13 November 2024

Revised: 10 January 2025

Accepted: 21 January 2025

Published: 26 January 2025

Citation: Nishimura, R.; Yamashita, M.; Murahata, Y.; Sunden, Y.; Tsuka, T. Diagnosis of Cystic Endometrial Hyperplasia and Hydrometra in a Pet Goat. *Ruminants* **2025**, *5*, 6. <https://doi.org/10.3390/ruminants5010006>

Copyright: © 2025 by the authors. Licensee MDPI, Basel, Switzerland. This article is an open access article distributed under the terms and conditions of the Creative Commons Attribution (CC BY) license (<https://creativecommons.org/licenses/by/4.0/>).

1. Introduction

Hydrometra is a common reproductive disease that causes infertility in goats [1]. This disease has been previously detected in 3.0 to 20.8% of sick or infertile female goats [1] and reported in 0.3 to 1.6% of pathological reproductive tracts obtained from goats slaughtered in abattoirs [2,3]. Persistent corpus luteum is a common cause of this disease [2,4–7], with pseudopregnancy being a well-known synonym for this disease [1,5–8]. Endometritis is considered a possible cause of the development of hydrometra in goats [9,10].

Hydrometra can also cause fluid evacuation through the vaginal valve, referred to as a cloudburst [2,4,5,7]. This disease can cause varying volumes of intrauterine effusions ranging between 0.25 and 8 L, resulting in the distention of the affected uterus [4]. The intrauterine fluids can be broadly divided into septic and aseptic effusions [2,5,11]. The intrauterine retention of aseptic effusions is a common characteristic of various uterine diseases observed in female goats [11]. In contrast, septic fluid accumulation enables the specific diagnosis of pyometra, a rare caprine uterine disease, accounting for 0.4 to 2.8% [3]. Hydrometra is a common aseptic disease that occurs worldwide [4–7]. Reproductive tract tumors are diagnosed in 4.0 to 8.7% of affected goats during necropsy [12]. Pet goats tend to have a higher prevalence of reproductive tract tumors than production animals because of their longer lifetimes [12]. Caprine cases with reproductive tract tumors tend to exhibit various clinical signs, such as vulvar discharge of hemorrhage, mucoid, or purulent materials, udder development, and abdominal distension [12]. These signal appearances are not specific for differentiating between tumor and non-tumor diseases, including endometritis, hydrometra, and pyometra [12,13]. Thus, the development of diagnostic techniques is required to differentiate between these uterine diseases for subsequent decisions regarding therapeutic options and prognosis.

In small animal practice, the clinical use of imaging modalities, such as radiography, ultrasonography, endoscopy, and computed tomography (CT), is essential for diagnosing various diseases of the urogenital organs, such as the ovary, oviduct, uterus, and vagina [14–17]. Various diseases in the reproductive tracts of small and large ruminants have previously been diagnosed using imaging modalities such as ultrasonography [2,3,5–8,11–13,18–23], radiography [24], CT [24,25], and intrauterine endoscopy (hysteroscopy) [10,14,26–30]. Although the diagnosis of hydrometra in goats is typically based on ultrasonographic observations, CT has not yet been used.

In previous cases, intramuscular injections of prostaglandin F₂α (PGF₂α) or oxytocin have been commonly administered for treatment, as the concurrent involvement of a persistent corpus luteum is common in most cases of caprine hydrometra [2,4–7]. However, a few patients respond poorly to these medical treatments [6,7,23]. In such cases, an ovariohysterectomy is a viable therapeutic approach used for pet goats if they do not need to be reproduced [4,31,32].

In this study, we aimed to present the clinical efficacy of the combined use of ultrasonography, CT, and hysteroscopy for diagnosing hydrometra, thereby contributing to improved surgical decisions and planning for pet goats.

2. Case Presentation

A 9-year-old Alpine mixed-breed pet female goat with 46.5 kg body weight presented with anestrus within the last 6 months, followed by gradual abdominal distention and continuous mucosal discharge. The present case had no history of delivery, as she was kept alone in the owner's house. An intramuscular injection of PGF₂α before admission resulted in a temporary discharge of endometrial fluids, followed by a recurrence of mucosal discharge. Activity and drinking were normal despite a decrease in appetite.

Blood examination: At admission, hematological examination revealed a slightly decreased red blood cell count ($680 \times 10^4/\mu\text{L}$, reference range: $800\text{--}1800 \times 10^4/\mu\text{L}$ [33]). No abnormal values were found in serum biochemistry. Plasma estradiol-17 β (E2) and progesterone (P4) concentrations were measured using an immunofluorescence assay kit (Mini Vidas; BioMérieux, Chemin de l'Orme, France). The plasma E2 and P4 levels were 41.9 pg/mL and 0.55 ng/mL on the initial clinical day, respectively (Table 1).

Table 1. Blood levels of estradiol-17 β and progesterone.

Variable	Initial Day	Day 14	Day 24	Reference Values
Estradiol-17 β (ng/mL)	41.9	23.4	25.9	16.5 (peak estrus phase) [19]
Progesterone (pg/mL)	0.55	18.34	0.51	3.6-4.3 (luteal phase) [34]

Ultrasonography: An ultrasound scanner (MyLabOne VET; Esaote Europe BV, Maastricht, Netherlands) was used to scan the animal in its standing position. The percutaneous application of a 2.5 MHz sector transducer to the caudal abdomen revealed an enlarged uterus within the lumen, which contained anechoic fluids (Figure 1).

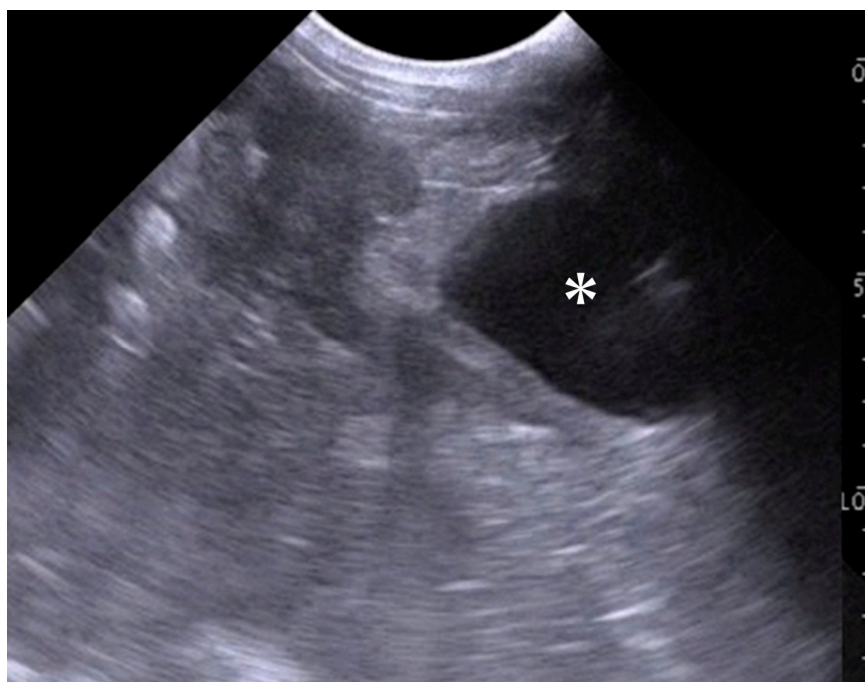


Figure 1. Ultrasonographic appearance of the uterus when scanning percutaneously. Anechoic fluid (asterisk) is seen within the enlarged uterine lumen. Scale = 10 mm.

CT: The animal was examined using a slip-ring CT scanner (Pronto SE; Hitachi Co. Ltd., Tokyo, Japan) while positioned in the lateral recumbency on the examination table under anesthesia after intravenous injection of xylazine hydrochloride (0.2 mg/kg; Selactar 2%; Bayer Yakuhin Ltd., Osaka, Japan). The transverse CT images obtained from scanning after intravenous injection of the contrast medium, iopamidol (2.0 mL/kg; Iopamirone 300mg/mL; Bayer Healthcare, Osaka, Japan), displayed a heterogeneously enhanced uterine mass. In this uterine mass, the right uterine horn appeared as a ball-like structure of approximately 5 cm in size at the basal area, and the uterine tube was also enlarged to a thickness of approximately 2 cm (Figure 2a). The lumen of the enlarged right uterine horn and uterine tube was unclear on the CT. The right ovary was approximately 2 cm in size and included a non-enhanced, round, follicle-like structure of a maximum of 10 mm. The

left uterine horn was enlarged to a thickness of approximately 3 cm. The structure of the left ovary was not evident on CT because it overlapped with the structure of the uterine horn. On the dorsal CT section of the caudal abdomen, the right uterine horn was thicker than the left (Figure 2b). No morphological or contrast-enhanced abnormalities were observed in other abdominal organs. No lymphadenopathy was evident in the abdominal cavity.

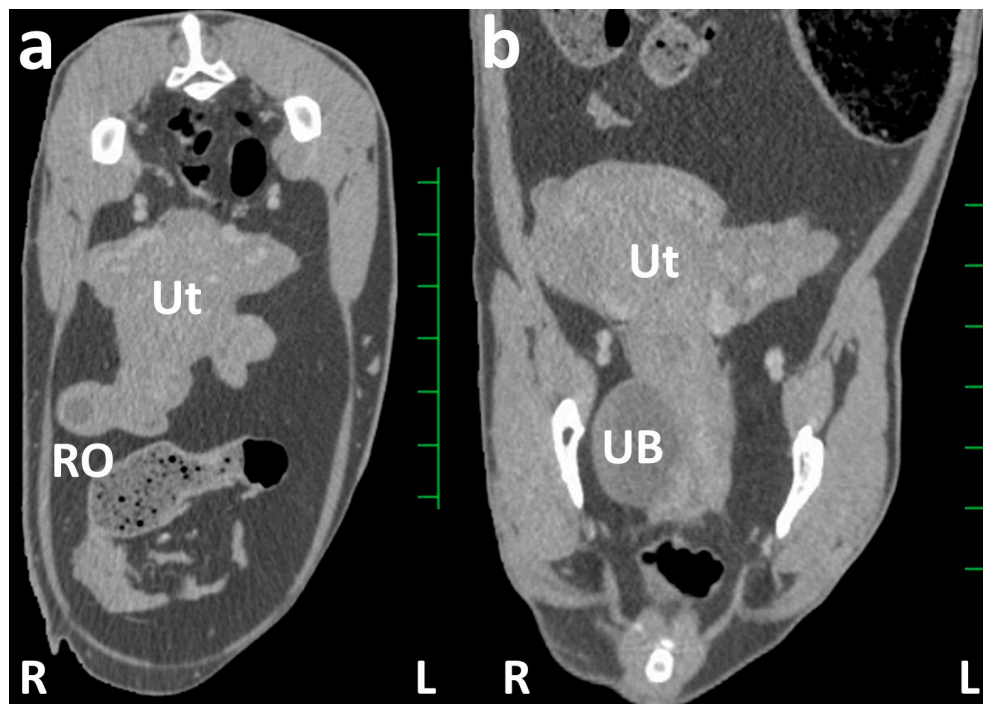


Figure 2. Transverse (a) and dorsal (b) contrast computed tomography images of the caudal abdomen. (a) The right uterine horn is shown as an enlarged, round structure, larger than that of the left uterine horn. The homogeneously contrast-enhanced structure represents the enlarged uterus (Ut), wherein the uterine lumen is unclear. The contrast-enhanced ball-like structure of the right ovary (RO) includes a round cystic structure with weak contrast enhancement. (b) The uterus (Ut) is represented as the enlarged uterine cervix running along the urinary bladder (UB) within the pelvic cavity, and the uterine horns extend to the location approximately 4 cm cranially compared with the pelvis. Scale = 25 mm.

Hysteroscopy: Under the same anesthetic condition, the animal was subsequently examined by hysteroscopy using a gastroscope (Fujifilm EG 530NP; outer diameter 4.9 mm and working channel 2.0 mm, Fujifilm Co., Tokyo, Japan) and a video processor (TC200EN; KARL STORZ Endoscopy Japan K.K., Tokyo, Japan). Under endoscopic observation, while moving the introduced endoscope toward the deep areas of the uterine lumen, a large amount of clear fluid content without turbidity accumulation was seen within the uterine lumen. The corrugated thickening of the endometrium was observed throughout the uterine lumen (Figure 3). Water flushing from the endoscope into the uterine lumen appeared to float in the endometrial corrugations, suggesting softer structures. The endometrial surfaces were pale pink without discoloration. The corrugated structures were collected using biopsy forceps (2.0 mm × 1150 mm; Olympus FB-211D, Olympus Medical Systems Co., Tokyo, Japan) and introduced through a working channel.

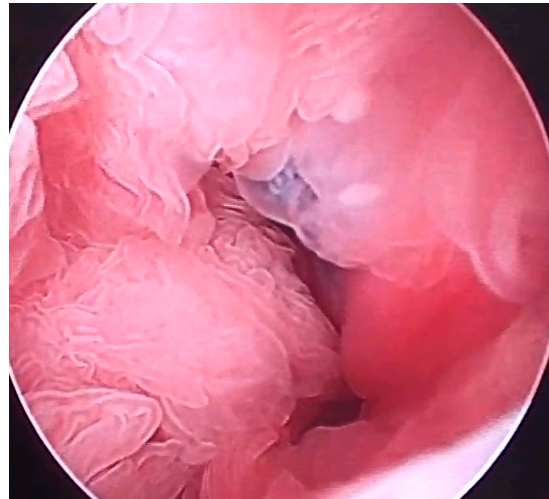


Figure 3. Hysteroscopic appearance of the uterus. Corrugation is evident in the whole area of the endometrial walls.

Hysteroscopy-assisted biopsy: Histopathological examination of the biopsy specimens revealed predominant edematous changes in the stroma and a slight hyperplasia of the uterine glands. There was infiltration of inflammatory cells, in which lymphocytes and plasma cells were predominant within the endometrial structures. No mitotic or tumor-like changes were observed. No bacterial aggregates were detected in the pathological examination. Based on these findings, the pathological changes in the endometrium were confirmed as chronic endometritis, although the etiological cause was unknown. Additionally, a comprehensive evaluation of the diagnostic and pathological results led to a diagnosis of hydrometra in the present case.

Surgery: On day 14, the goat underwent an ovariohysterectomy. Inhalation anesthesia was obtained with 2–3% isoflurane (ds isoflurane; DS Pharma Animal Health Co., Ltd., Osaka, Japan) via a tracheal tube inserted after anesthesia with intravenous injection of xylazine hydrochloride (0.2 mg/kg) and butorphanol (0.2 mg/kg; Vetorphale, Meiji Seika Pharma Co., Ltd., Tokyo, Japan), followed by a one-shot injection of propofol (2 mg/kg; Propoflo 28; Zoetis, Parsippany, NJ, USA). A skin incision of 15 cm was made along the ventral abdominal midline of the anesthetized dorsal recumbent animal. A severely extended uterus was detected within the abdominal cavity through the surgical opening of the abdominal wall. Macroscopically, the uterus was observed as multiple-beaded extended parts aligned on its tubular structure (Figure 4a). The right uterine horn appeared larger than the left. The left ovary, approximately 1 cm in size, was found behind the left uterine horn (Figure 4b). The ovarian ligament, including the ovarian artery and vein, was cut after suturing these vessels with a monofilament absorbable suture (Ethicon PDS II USP 2-0; Johnson & Johnson K.K., New Brunswick, NJ, USA). In the apex of the round, enlarged right uterine horn, the right ovary, approximately 2 cm in size, and the thickened uterine tube were observed (Figure 4c). Macroscopically, the follicular and luteal structures were present within the parenchyma of the right ovary. The ovarian ligament was cut similarly to that of the left ovary. An incision was made in the broad ligament of the uterus attached anatomically to both sides of the uterine body after the ligation of the blood vessels along their membranous structures. The uterine arteries running along both edges of the thickened uterine cervix were ligated, followed by the ligation of the body of the uterine cervix using an absorbable suture material (MAXON; Davis and Geck Inc., Brooklyn, NY, USA) (Figure 4d). Subsequently, an incision was made cranially at the location of the uterine cervix, leading to complete resection of the uterine body (Figure 4e). The cut surface of the uterine cervix was closed using purse-string suturing, followed by

Lembert suturing using an absorbable suture material (Figure 4f). The abdomen was closed by running suturing to the peritoneum and muscular layers using an absorbable suture material, followed by suturing to the incised skin using a nylon suture material (Suprylon USP0, Vömel, Gronberg, Germany).

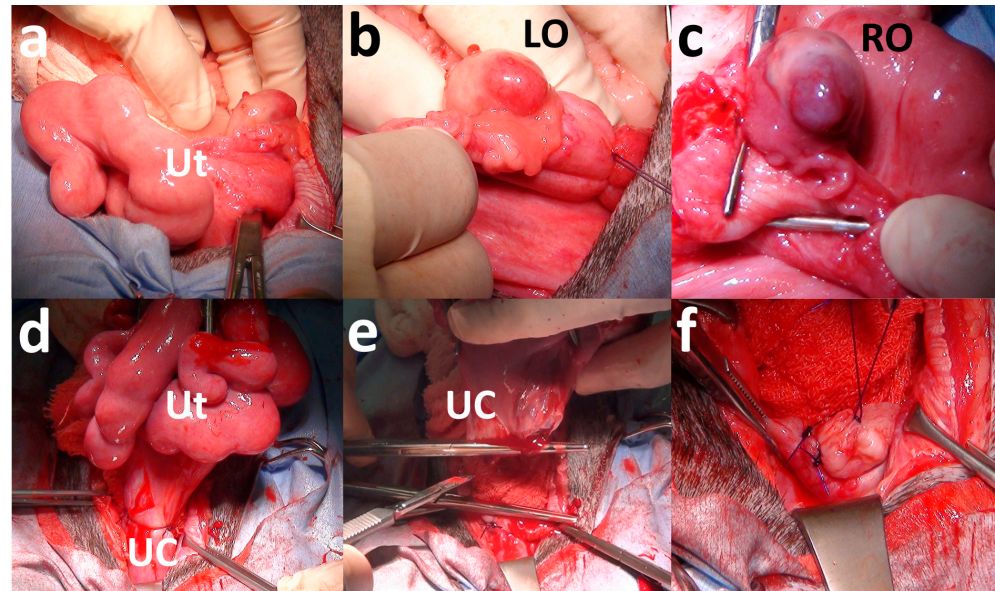


Figure 4. Images of the surgical procedure of ovariectomy. (a) The multiple-beaded, extended uterus (Ut) is seen when pulled out from the abdominal cavity. (b) The left ovary (LO), approximately 1 cm in size, is located behind the left uterine horn. The corpus luteum is seen in the LO. (c) The right ovary (RO), approximately 2 cm in size, has follicular and luteal structures. (d) The severely thickened uterine cervix (UC) is seen when the uterus (Ut) is held out of the abdominal cavity. (e) An incision is made in the UC after its ligation. (f) The cut surface of the UC is closed with purse-string suturing.

Follow-up: The animal was treated with intramuscular administrations of a streptomycin–penicillin complex for 3 days (Mycillin; Meiji Seika Pharma Co. Ltd., Tokyo, Japan). On day 24 (10th postoperative day), the animal exhibited satisfactory postoperative outcomes without complications, including no discharge from the vulva, despite a slight swelling of the sutured skin. There was no recurrence of reproductive disturbances. The plasma levels of E2 and P4 were 23.4 pg/mL and 18.34 ng/mL, respectively, in the blood samples obtained preoperatively on day 14 (Table 1). On postoperative day 10, the plasma E2 levels (25.9 pg/mL) did not decrease significantly compared with those on the initial clinical day and day 14.

Macroscopic and pathological examinations: Within the lumen of the uterus removed surgically, the endometrial walls exhibited a diffuse thickening because of swelling, and multiple cystic changes were macroscopically observed (Figure 5a). Histologically, the cyst wall lining comprised one or two layers of cuboidal or flat epithelial cells. The muscular layers were thinner and included proliferating uterine glands. The proliferation of stromal cells was observed along the underlying layers of the mucosal epithelium (Figure 5b). Adenomyosis was observed in the uterine horn. Some corpora lutea were observed in cut sections of both ovaries (Figure 5c). Histologically, multiple formations of cystic structures lined with granulosa cells within the cortex were observed (Figure 5d). The cyst wall was lined with granulosa cells and contained certain inflammatory cells, such as macrophages, lymphoid cells, and some cell debris (desquamated cells), suggestive of follicular cysts. Furthermore, luteal cells comprising small and large cells, predominantly and partly referred to as theca lutein and granulosa lutein cells, respectively, were found in both

ovaries. Granulosa lutein cells were strongly acidophilic and showed atrophic changes, suggesting a mild degenerative change.

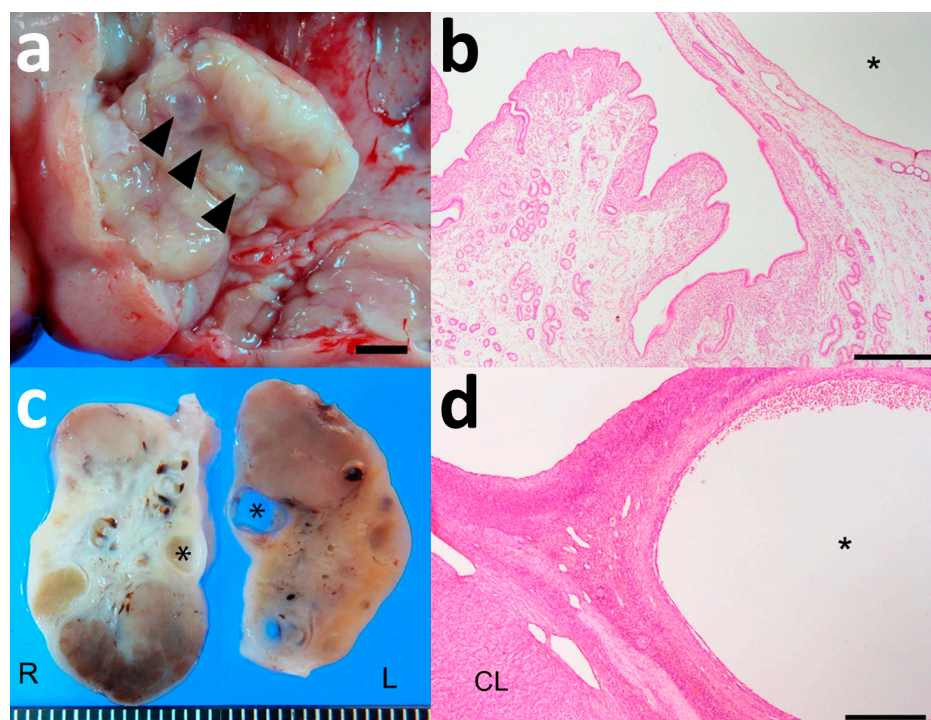


Figure 5. Surgically removed uterus and ovaries. (a) Swelling of the uterine mucosa and multiple cystic formations (arrowheads) are noted. Scale bar = 5 mm. (b) A cyst (asterisk) located in the endometrium is lined by a few layers of epithelial cells. The proliferation of stromal cells and marked edematous changes can be seen in the submucosa. Bar = 500 µm. (c) The cut surface of ovaries after formalin fixation. Both ovaries contain multiple corpus luteum (yellow to brownish nodules) and a few cystic structures (asterisks). Scale represents 1 mm intervals. (d) In the cortex of the ovary, a cyst (asterisk) is lined by granulosa cells and contains some cell debris. Bar = 500 µm.

3. Discussion

In the present case, the combined use of ultrasonography, CT, and hysteroscopy was extremely helpful in diagnosing hydrometra and ovarian follicular cysts, guiding the decision to perform an ovariectomy. In the diagnostic process using these modalities, the present case was initially examined using ultrasonography while scanning percutaneously via the abdominal wall. Transabdominal ultrasonographic scanning was chosen because the patient did not have a large enough body mass for the transrectal approach [7,18]. The transrectal scanning of small animals can lead to rectal damage [35]. Transabdominal scanning may be inferior to transrectal scanning in the visibility of the reproductive organs, possibly because of the differences in the ultrasound frequency of the applicable transducer, as previously ranging between 3.0 and 6.5 MHz [2,5,11,19,21–23] and between 5.0 and 10.0 MHz [6–8,11,13,18,20,21], respectively. Additionally, it is challenging to demonstrate the whole structures of the reproductive organs using transabdominal scanning. This may have limited the diagnostic information obtained by ultrasonography in the present case. Transvaginal ultrasonography could have been utilized as the alternative scanning method to demonstrate the pathological reproductive tract because it has previously helped the identification of early pregnant uteruses in goats [36].

The previous applications of ultrasonography for sick or infertile female goats could help identify the varying prevalence of hydrometra, accounting for 1.4 to 51.0% [5–8,21]. The ultrasonographic observations of this disease are characterized by varying amounts

of anechoic fluids within the uterine lumen, where small hyperechoic deposits float occasionally [5,7,10,11,21,35]. The echogenicity of the intrauterine effusion was higher on the ultrasonogram of pyometra than that of hydrometra and endometritis [10,11,22]. However, differentiating hydrometra from pyometra may occasionally be difficult [35] because of the varying echogenicity of intrauterine effusion, which appears anechoic [6,7] to hypoechoic [8]. Additionally, the ultrasonographic findings of hydrometra showing small amounts of intrauterine effusion can be misdiagnosed as early pregnancy when the echotextures of the fetus and placentome cannot be found [7,35]. In terms of the ultrasonographic appearances of uterine tumors compared with those of hydrometra, these uterine diseases can be differentiated based on the ultrasonographic findings observed in half of the previous caprine cases, including the formation of hyperechoic mass structures derived from the endometrium and muscular layers and multifocal, anechoic, cystic lesions diffused within uterine walls [12,13,19]. However, intrauterine fluid retention was the common ultrasonographic finding among these uterine diseases, as reported in 38% of examined caprine cases with uterine tumors [12,13,19]. Thus, using ultrasonography alone makes it difficult to distinguish common uterine diseases [10].

Previous clinical use of CT for diagnosing caprine urogenital diseases has rarely been reported [24,25], despite a few previous reports describing the anatomical evaluation of abdominal CTs in goats [20]. In the CT scans of the caudal abdomen and pelvis, where the narrow cavities are fully crammed with the reproductive tract, the urinary system, colon, and rectum can be identified as separate structures without an overlap in two-dimensional CT sections [20,37]. CT can provide basic transverse cross-sectional images, enabling the reconstruction of every directional plane and a three-dimensional image [20,37]. Reconstructed sagittal CT planes can contribute effectively to evaluating the extent of masses that spread between the abdominal and pelvic cavities and the positional relationship of pathological uterine and ovarian structures against the peripheral organs [25,38]. Detecting the systemic formation of metastatic foci and lymphadenomegaly during whole-body scanning using CT can lead to diagnostic suggestions for neoplastic lesions [24,25]. The CTs of reproductive tract lesions can be evaluated quantitatively by measuring lesion size and Hounsfield units [37]. In the present case, the CT-based measurement of ovarian follicle size within the right ovary helped diagnose a follicular cyst based on the ultrasonographic criteria of follicular cysts [3,7,11,21]. These cysts were >10 mm in size [3,7,11,21], compared with 8–9 mm of the maximum size of a follicle formed within the ovary in the estrous cycle of female goats [11,18]. Contrast techniques for radiographic examination are applicable to CT scanning [25,38,39]; these techniques include excretory urography, retrograde cystography [38], hysterothorography, identifying the pathological enlargements of the affected uterus and fertile states [14,16], and vaginography, helping in diagnosing ectopic ureters and urethrovaginal and rectovaginal fistulas [15,39]. The intravenous injection of contrast medium during CT scanning can provide significant evidence of contrast enhancement, such as the difference in contrast-enhanced density within the lesions and the time required for contrast enhancement [24]. Contrast enhancement and fluid retention within the uterine lumen are significant CT features that differentiate between neoplastic and non-neoplastic uterine diseases [25]. In the present case, contrast CT revealed that the thickened uterine walls were occupied predominantly by a fluid retention area within the enlarged uterine structure.

Hysteroscopy is routinely used for intrauterine catheterization and artificial insemination in goats [27,40]. In the present case, hysteroscopy was performed under deep anesthesia for CT examination before the procedure. Hysteroscopy has been performed in previously examined bovine, buffalo, equine, and caprine cases in their standing position, with or without sedation [27–30,41]. Epidural anesthesia is required when hysteroscopy is

performed in unanesthetized animals [27–30]. The applicable diameters of endoscopes to be introduced into the uterine lumen of examined goats have ranged from 5.0 to 5.5 mm [10,30]. The smaller diameter of an endoscope (e.g., 2 mm) may be recommended for application in female caprine cases, based on a previous practical record wherein the intrauterine introduction of the larger diameter of the endoscope was faulty in 55.8% of uteri if incision in the cervix was not made [10,40]. The intrauterine infusions of sterile saline or lactated Ringer's solution can lead to the distention of the uterine lumen, contributing to good endoscopic observations [30]. Flushing of the uterine lumen was performed in the same manner as in the present case, allowing for the observation of color and turbidity of the intrauterine effusion and subsequent cytological and bacteriological examinations, although the stirred mucopurulent materials could cause unclearness in the hysteroscopic view in the previous cases [30]. Endometritis is a common uterine disease for which hysteroscopy is preferred [10,29,30]. The previous use of hysteroscopy in sick female goats enabled the identification of endometritis in 45.2% of cases, followed by the detection of endometrial hemorrhages, hydrometra, mucometra, and pyometra in 19.4, 16.1, 9.9, and 9.7% cases, respectively [10]. The common hysteroscopic appearances of endometritis are the discoloration and thickening of the endometrial walls of the affected uterus, whereas ultrasonography enables the demonstration of only endometrial thickening [10,26,29]. Additionally, the corrugation of thickened endometrial walls can be commonly identified in hysteroscopic observations [29], similar to that in the present case. Hysteroscopy-assisted biopsy was successfully performed to identify endometritis preoperatively in the present case. Thus, this technique is the most optimal approach for hysteroscopy, which has also been performed in previous caprine cases [9,27,28]. Under hysteroscopic observations, biopsy specimens can be selectively collected from the pathological surface of the endometrium, identified based on discoloration and ulceration, using pilling biopsy forceps [16,17,41]. The hysteroscopic detection of endometritis can consequently contribute to the diagnosis of hydrometra because these uterine lesions mostly occur concurrently in affected female goats [9,10].

The most common therapeutic option for small ruminants when diagnosed with hydrometra is the administration of PGF2 α [2,5–7,23]. However, a few treated animals do not exhibit complete resolution of clinical signs, and a single administration of PGF2 α has been reported to result in the recurrence of hydrometra in 45% of treated animals [6,7,23]. No pharmacological interventions, including PGF2 α and oxytocin, have previously yielded therapeutic evidence to decide for laparotomy or laparoscopy as the treatment that needs to be performed subsequently [4,31,32]. For pet goats, surgery must be actively selected to maintain an adequate quality of life and improve undesirable, aggressive behaviors [31,32]. In previous cases of caprine and ovine hydrometra treated with ovariohysterectomy, the removed uteri typically included a large amount of intrauterine effusion measured between 1.5 and 6.5 L [2,4,31]. Endometrial stromal polyp formation was rarely detected in a previous caprine case [19]. Thus, surgical planning can be supported by preoperative CT findings to evaluate varying pathological conditions, such as uterine size and degree of fluid retention in the affected uterus. For example, in the present case, the CT-based preoperative findings indicated that endometrial proliferation was the predominant uterine lesion.

In the present case, the higher plasma E2 concentration on the initial clinical day (41.9 pg/mL) seemed to correspond to the CT and macroscopic results, in which an enlarged ovary included a follicular cyst [42]. The involvement of this ovarian lesion was consistent with the histopathological results showing accelerated mucosal secretion from the hyperplastic endometrium. Thus, the present case was considered to involve hydrometra induced by a follicular cyst [7,22]. The increased blood levels of estrogen were measured

as 13.6 and 31.8 pg/mL on average in previous caprine cases affected with hydrometra and endometritis, respectively [7,22]. In the present case, hyperestrogenism may have promoted favorable conditions for the development of endometritis, potentially serving as a primary cause of hydrometra [4]. However, a normal ovarian cycle in the present case could not be completely denied because plasma P4 concentrations over a period of the examined time seemed to be changed within the common levels measured during the follicular and luteal phases [42]. It has not been well known whether the luteal structures observed macroscopically within both ovaries were functional or persistent corpus luteum, whereas a persistent corpus luteum might be doubtful because of the lack of a therapeutic effect of PGF2 α administration, as this treatment targets this condition, one of the typical causes of hydrometra [2,4–7]. Relatively high plasma E2 levels were maintained after ovariectomy in the present case. However, the extragonadal source of E2 in goats is not clearly understood. In rats, blood E2 concentrations have been reported to increase gradually until 4 months after ovariectomy [43]. The increase in extragonadal E2 production may depend on the expression of aromatase enzyme in the liver and adipose tissues and the increased adrenal expression of P450c17, which converts P4 to testosterone until 6 months after ovariectomy [43]. This extragonadal E2 production may also have functioned in the present case, as the adrenal gland is known as the principal organ for producing sex steroids, except for the ovary, in female goats [44].

4. Conclusions

Based on the clinical results of the present case, it can be concluded that hydrometra in goats can be accurately diagnosed by the combined use of various imaging modalities, including transabdominal ultrasonography for providing initial, suggestive evidence of uterine disease, if any; CT for enabling multiple evaluations for extension degree and the contrast enhancement of the affected uterus; and hysteroscopy leading to macroscopic intrauterine observation of pathological endometrial changes and effusion retention, followed by the use of hysteroscopy-assisted biopsy. The advanced diagnostic technique commonly utilized in small animal practice can be applied to pet goats with various urogenital diseases, whereas the clinical use of this technique would be difficult on livestock farms because of the examination cost and lack of inspection institute.

Author Contributions: Conceptualization, R.N. and T.T.; methodology, R.N., M.Y., Y.M., Y.S. and T.T.; writing—review and editing, R.N. and T.T. All authors have read and agreed to the published version of the manuscript.

Funding: This research received no external funding.

Institutional Review Board Statement: We have not gotten approval code for this case, because this case was a patient, but not an experimental animal. On the other hand, the study protocol was performed in accordance with an ethical approval information: (https://assets.publishing.service.gov.uk/government/uploads/system/uploads/attachment_data/file/388535/CoAnimalsWeb.pdf, accessed on 20 January 2025).

Informed Consent Statement: We obtained informed written consent from the owner, which covered the usefulness of ultrasonography, CT and hysteroscopy in differential diagnosis of this reproductive disease, and the requirement of surgical therapy for complete recovery.

Data Availability Statement: The data presented in this study are available on request from the corresponding author.

Conflicts of Interest: The authors declare no conflict of interest.

References

1. Hesselink, J.W. Incidence of hydrometra in dairy goats. *Vet. Rec.* **1993**, *132*, 110–112. [[CrossRef](#)] [[PubMed](#)]
2. Pieterse, M.C.; Taverne, M.A.M. Hydrometra in goats: Diagnosis with real-time ultrasound and treatment with prostaglandins or oxytocin. *Theriogenology* **1986**, *26*, 813–821. [[CrossRef](#)]
3. Reddy, K.C.S.; Reddy, V.S.C.; Rao, A.S.; Reddy, J.M.; Sharma, G.P. Studies on the incidence of reproductive abnormalities in local non-descript female goats. *Indian J. Anim. Reprod.* **1997**, *18*, 51–53.
4. Pfister, P.; Geissbuehler, U.; Wiener, D.; Hirsbrunner, G.; Kaufmann, C. Pollakisuria in a dwarf goat due to pathologic enlargement of the uterus. *Vet. Q.* **2007**, *29*, 112–116. [[CrossRef](#)] [[PubMed](#)]
5. Purohit, G.N.; Mehta, J.S. Hydrometra in goats (*Capra hircus*): Clinical analysis of 26 cases. *Rumin. Sci.* **2012**, *1*, 117–119.
6. Barna, T.; Apić, J.; Bugarski, D.; Maksimović, N.; Mašić, A.; Novaković, Z.; Milovanović, A. Incidence of hydrometra in goats and therapeutic effects. *Arch. Vet. Med.* **2017**, *10*, 13–24. [[CrossRef](#)]
7. Maia, L.R.S.; Brandão, F.Z.; Souza-Fabjan, J.M.G.; Veiga, M.O.; Balara, M.F.A.; Siqueira, L.G.B.; Facó, O.; Fonseca, J.F. Hydrometra in dairy goats: Ultrasonic variables and therapeutic protocols evaluated during the reproductive season. *Anim. Reprod. Sci.* **2018**, *197*, 203–211. [[CrossRef](#)] [[PubMed](#)]
8. Moraes, E.A.; Santos, M.H.B.; Arruda, I.A.; Bezerra, F.A.; Aguiar, C.; Neves, J.P.; Lima, P.F.; Oliveira, M.A.L. Hydrometra and mucometra in goats diagnosed by ultrasound and treated with PGF2. *Med. Veterinária Recife* **2007**, *1*, 33–39.
9. Radi, Z.A. Endometritis and cystic endometrial hyperplasia in a goat. *J. Vet. Diagn. Investig.* **2005**, *17*, 393–395. [[CrossRef](#)] [[PubMed](#)]
10. Kumar, P.; Dholpuria, S.; Purohit, G.N. Hysteroscopic and ultrasonographic evaluation of goat (*Capra hircus*) uterus. *J. Entomol. Zool. Stud.* **2020**, *8*, 1108–1112.
11. Gonzalez-Bulnes, A.; Pallares, P.; Vazquez, M.I. Ultrasonographic imaging in small ruminant reproduction. *Reprod. Domest. Anim.* **2010**, *45*, 9–20. [[CrossRef](#)] [[PubMed](#)]
12. Linton, J.K.; Heller, M.C.; Bender, S.J.; Stefanovski, D.; Fecteau, M.E. Neoplasia of the tubular genital tract in 42 goats. *J. Am. Vet. Med. Assoc.* **2020**, *256*, 808–813. [[CrossRef](#)] [[PubMed](#)]
13. Dockweiler, J.C.; Cossic, B.; McDonough, S.P.; Fubini, S.L.; Le, K.M.; Donnelly, C.G.; Gilbert, R.O.; Cheong, S.H. Tumor collision of uterine adenocarcinoma and leiomyosarcoma in a goat. *J. Vet. Diagn. Investig.* **2017**, *29*, 696–699. [[CrossRef](#)] [[PubMed](#)]
14. Lagerstedt, A.S.; Obel, N.; Stavenborn, M. Uterine drainage in the bitch for treatment of pyometra refractory to prostaglandin F2 α . *J. Small Anim. Pract.* **1987**, *28*, 215–222. [[CrossRef](#)]
15. Rivers, B.; Johnston, G.R. Diagnostic imaging of the reproductive organs of the bitch. Methods and limitations. *Vet. Clin. N. Am. Small Anim. Pract.* **1991**, *21*, 437–466. [[CrossRef](#)] [[PubMed](#)]
16. Watts, J.R.; Wrigh, P.J. Investigating uterine disease in the bitch: Uterine cannulation for cytology, microbiology and hysteroscopy. *J. Small Anim. Pract.* **1995**, *36*, 201–206. [[CrossRef](#)] [[PubMed](#)]
17. Fontaine, E.; Levy, X.; Grellet, A.; Luc, A.; Bernex, F.; Boulouis, H.J.; Fontbonne, A. Diagnosis of endometritis in the bitch: A new approach. *Reprod. Domest. Anim.* **2009**, *44* (Suppl. 2), 196–199. [[CrossRef](#)] [[PubMed](#)]
18. de Castro, T.; Rubianes, E.; Menchaca, A.; Rivero, A. Ovarian dynamics, serum estradiol and progesterone concentrations during the interovulatory interval in goats. *Theriogenology* **1999**, *52*, 399–411. [[CrossRef](#)] [[PubMed](#)]
19. Eljarah, A.; Sod, G.; Gill, M.; Lyle, S.; Taylor, W. Bloody vaginal discharge in a goat with an endometrial stromal polyp. *Large Anim. Rev.* **2012**, *18*, 317–319.
20. Alnahrawy, E.H.; Rashed, R.; Shogy, K.; Erasha, A. Morphological and diagnostic imaging studies on pelvic cavity of Egyptian female Baladi goat (*Capra hircus*). *J. Curr. Vet. Res.* **2021**, *3*, 32–40. [[CrossRef](#)]
21. Balara, M.F.A.; Cosentino, I.O.; Ribeiro, A.C.S.; Brandão, F.Z. Ultrasound diagnosis in small ruminants: Occurrence and description of genital pathologies. *Vet. Sci.* **2022**, *9*, 599. [[CrossRef](#)] [[PubMed](#)]
22. Khamees, H.A.; Alsalim, H.A.; Abbas, M.F.; Hameed, W.S. Ultrasonographical and hormonal study on some causes of infertility in Iraqi goats (*Capra hircus*). *IAR J. Agric. Res. Life Sci.* **2023**, *4*, 19–25.
23. Hesselink, J.W. Hydrometra in dairy goats: Reproductive performance after treatment with prostaglandins. *Vet. Rec.* **1993**, *133*, 186–187. [[CrossRef](#)]
24. Stieger-Vanegas, S.M.; McKenzie, E. Imaging of the urinary and reproductive tract in small ruminants. *Vet. Clin. N. Am. Food Anim. Pract.* **2021**, *37*, 75–92. [[CrossRef](#)] [[PubMed](#)]
25. Collins-Webb, A.G.; Löhr, C.V.; Stieger-Vanegas, S.M. CT features of malignant tubular genital tract tumors in seven goats. *Vet. Radiol. Ultrasound* **2023**, *64*, 253–261. [[CrossRef](#)]
26. Madoz, L.V.; De La Sota, R.L.; Susuki, K.; Heuviser, W.; Drillich, M. Use of hysteroscopy for the diagnosis of postpartum clinical endometritis in cows. *Vet. Rec.* **2010**, *167*, 142–143. [[CrossRef](#)]
27. Shao, C.Y.; Wang, H.; Meng, X.; Zhu, J.Q.; Wu, Y.Q.; Li, J.J. Characterization of the innate immune response in goats after intrauterine infusion of *E. coli* using histopathological, cytologic and molecular analyses. *Theriogenology* **2012**, *78*, 593–604. [[CrossRef](#)]

28. Shao, C.; Wang, H.; Wang, X.; Jiang, S.; Sun, J.; Song, H.; Li, J. Characterization of inflammatory responses by cervical cytology, cytokine expression and ultrastructure changes in a goat subclinical endometritis model. *J. Vet. Med. Sci.* **2017**, *79*, 197–205. [[CrossRef](#)] [[PubMed](#)]
29. Chaudhary, V.; Jeengar, K.; Ruhil, S.; Purohit, G.N. Efficiency of hysteroscopic visualization of bubaline uterus. *Anim. Reprod. Sci.* **2014**, *149*, 353–355. [[CrossRef](#)]
30. Purohit, G.N.; Gaur, M.; Chaudhary, A.K.; Thanvi, P.; Saraswat, C.S.; Dholpuria, S. Prospects of hysteroscopy in large domestic animals: A mini review. *J. Entomol. Zool. Stud.* **2020**, *8*, 466–469.
31. Brabant, O.; Laurence, M. Surgical correction of four cases of hydrometra in ewes. *Vet. Rec. Case Rep.* **2017**, *5*, e000555. [[CrossRef](#)]
32. Daniel, A.J.; Easley, J.T.; Holt, T.N.; Griffenhagen, G.M.; Hackett, E.S. Laparoscopic ovariohysterectomy in goats. *J. Am. Vet. Med. Assoc.* **2019**, *254*, 275–281. [[CrossRef](#)]
33. Al-Bulushi, S.; Shawaf, T.; Al-Hasani, A. Some hematological and biochemical parameters of different goat breeds in Sultanate of Oman “A preliminary study”. *Vet. World* **2017**, *10*, 461–466. [[CrossRef](#)] [[PubMed](#)]
34. Fonseca, J.F.; Maffili, V.V.; Rodrigues, M.T.; Santos, A.D.F.; Rovay, H.; Pinto Neto, A.; Brandão, F.Z.; Torres, C.A.A. Effects of hCG on progesterone concentrations and fertility in cyclic, lactating Alpine goats. *Anim. Reprod.* **2006**, *3*, 410–414.
35. Hesselink, J.W.; Taverne, M.A.M. Ultrasonography of the uterus of goats. *Vet. Q.* **1994**, *16*, 41–45. [[CrossRef](#)] [[PubMed](#)]
36. Koker, A.; Ince, D.; Sezik, M. The accuracy of transvaginal ultrasonography for early pregnancy diagnosis in Saanen goats: A pilot study. *Small Rumin. Res.* **2012**, *105*, 277–281. [[CrossRef](#)]
37. Morita, Y.; Sugiyama, S.; Tsuka, T.; Okamoto, Y.; Morita, T.; Sunden, Y.; Takeuchi, T. Diagnostic efficacy of imaging and biopsy methods for peritoneal mesothelioma in a calf. *BMC. Vet. Res.* **2019**, *15*, 461. [[CrossRef](#)]
38. Le, K.; Wai, S.; Righter, B.; Weber, K.; Ruppert, S. Multiple urogenital abnormalities and urine incontinence in a sexually ambiguous goat (*Capra aegagrus hircus*). *Vet. Rec. Case Rep.* **2024**, *12*, e898. [[CrossRef](#)]
39. Botsikas, D.; Pluchino, N.; Kalovidouri, A.; Platon, A.; Montet, X.; Dallenbach, P.; Poletti, P.A. CT vaginography: A new CT technique for imaging of upper and middle vaginal fistulas. *Br. J. Radiol.* **2017**, *90*, 20160947. [[CrossRef](#)] [[PubMed](#)]
40. Colagross-Schouten, A.; Allison, D.; Brent, L.; Lissner, E. Successful use of endoscopy for transcervical cannulation procedures in the goat. *Reprod. Domest. Anim.* **2014**, *49*, 909–912. [[CrossRef](#)] [[PubMed](#)]
41. Card, C.E.; Eaton, S.; Ghasemi, F. How to perform a hysteroscopically assisted endometrial biopsy and foreign body retrieval in mares. *Proc. Am. Assoc. Equine Pract.* **2010**, *56*, 328–330.
42. Bono, G.; Cairoli, F.; Tamanini, C.; Abrate, L. Progesterone, estrogen, LH, FSH and PRL concentrations in plasma during the estrous cycle in goat. *Reprod. Nutr. Dev.* **1983**, *23*, 217–222. [[CrossRef](#)] [[PubMed](#)]
43. Zhao, H.; Tian, Z.; Hao, J.; Chen, B. Extragenadal aromatization increases with time after ovariectomy in rats. *Reprod. Biol. Endocrinol.* **2005**, *3*, 6. [[CrossRef](#)]
44. Meikle, A.W.; Daynes, R.A.; Araneo, B.A. Adrenal androgen secretion and biologic effects. *Endocrinol. Metab. Clin. N. Am.* **1991**, *20*, 381–400. [[CrossRef](#)]

Disclaimer/Publisher’s Note: The statements, opinions and data contained in all publications are solely those of the individual author(s) and contributor(s) and not of MDPI and/or the editor(s). MDPI and/or the editor(s) disclaim responsibility for any injury to people or property resulting from any ideas, methods, instructions or products referred to in the content.